Article

Effect of Cryo-Milling on PLA/CNC and PLA/Calcium Carbonate Nanocomposites: A Comparison Study

Fatemeh Mahdiyeh Boroujeni and Ronald Kander *

Posted Date: 14 April 2025

doi: 10.20944/preprints202504.1143.v1

Keywords: Cellulose nano crystals (CNC); Calcium Carbonate (CaCO3); Poly Lactide acid (PLA); Biocomposite; Dispersion; Mixing Methods; Cryo-milling; Hemp; Sustainability

 doi:10.20944/preprints202504.1143.v1

Article

Effect of Cryo-Milling on PLA/CNC and PLA/Calcium Carbonate Nanocomposites: A Comparison Study

Fatemeh Mahdiyeh Boroujeni and Ronald Kander*

School of Design and Engineering, Kanbar College, Thomas Jefferson University, Philadelphia, PA 19144, USA

* Correspondence: ronald.kander@jefferson.edu

Abstract: This study examines a new approach for improving the dispersion of hydrophilic fillers into a hydrophobic polymer matrix, a long-standing challenge that often limits the thermal and mechanical performance of biocomposites. We investigated two different types of fillers—natural cellulose nanocrystals (CNC) and mineral calcium carbonate ($CaCO_3$)—introduced into polylactic acid (PLA) at five different volume fractions. PLA-based biocomposite films were fabricated using physical mixing and cryo-milling methods, followed by hot pressing to study their effects. Cryo-milling was explored as a promising strategy to enhance filler distribution within the matrix. Thermal properties, crystallization behavior, and mechanical performance were characterized using differential scanning calorimetry (DSC), thermogravimetric analysis (TGA), and tensile testing. CNC addition slightly lowered the glass transition temperature (Tg), while $CaCO_3$ raised it; both fillers promoted crystallization, although overall crystallinity remained relatively stable. Mechanically, tensile strength and strain decreased with filler addition, but CNC composites, particularly those prepared by cryo-milling, retained better ductility. Both CNC and $CaCO_3$ increased the modulus of PLA composites, with $CaCO_3$ providing a greater improvement. Although cryo-milling improved nanoparticle dispersion within the PLA matrix, better interfacial bonding is still needed. Future strategies, such as surface modification of fillers—like PEG-coating CNC—are recommended alongside improved mixing methods to optimize composite performance for sustainable applications.

Keywords: Cellulose nano crystals (CNC); Calcium Carbonate (CaCO3); Poly Lactide acid (PLA); Biocomposite; Dispersion; Mixing Methods; Cryo-milling; Hemp; Sustainability

1. Introduction

Polylactic acid (PLA) is a biodegradable polymer widely recognized for its renewability, high-quality mechanical properties, and processability, making it suitable for high-value applications such as packaging, biomedical devices, and automotive components where sustainability is prioritized [1,2]. PLA is derived from renewable resources like corn starch and sugarcane, offering a significant advantage over petroleum-based polymers [3]. Additionally, PLA exhibits high tensile strength and transparency, making it versatile for numerous industrial uses [4]. However, PLA suffers from intrinsic limitations such as brittleness, low thermal stability, and inadequate strength, restricting its application in high-demand areas [5]. Improving these properties is crucial for its broader adoption, particularly in applications requiring high-performance materials.

To address PLA's limitations, reinforcing agents such as cellulose nano and microcrystals (CNC and CMC) and cellulose nanofiber have emerged as viable options [6]. These particles exhibit outstanding properties, including high mechanical strength (Young's modulus of 100–220 GPa), low density (1.5–1.6 g/cm^3), and exceptional biodegradability [7]. They also possess a high aspect ratio, making them suitable for improving polymer matrices' tensile and thermal performance [8].

 doi:10.20944/preprints202504.1143.v1

Additionally, cellulose whiskers' renewable and non-toxic nature aligns well with the growing demand for sustainable materials [9].

Despite these advantages, incorporating these particles into PLA poses significant challenges due to PLA's hydrophobic nature. Hydrophilic fillers often agglomerate within the PLA matrix, leading to weak interfacial bonding and non-uniform dispersion, adversely affecting the composite's mechanical and thermal performance [10–12]. Cryo-milling, a technique involving grinding at cryogenic temperatures, has addressed this issue by achieving finer particle sizes and uniform dispersion of CNC/CMC in the PLA matrix. This approach was benchmarked against traditional physical mixing methods to evaluate its efficacy in improving composite properties [13].

As a mineral control filler, calcium carbonate ($CaCO_3$), widely used in industrial composites, was incorporated [14]. While $CaCO_3$ is cost-effective and enhances stiffness, its inability to improve ductility or biodegradability makes it less suitable for sustainable applications [15,16]. In contrast, CNC/CMCs derived from hemp offer a fully bio-based reinforcement [17]. Hemp fibers, known for their high cellulose content (70–80%), were treated using citric acid hydrolysis. This process enhances CNC/CMC thermal and mechanical stability while minimizing environmental toxicity compared to traditional sulfuric acid hydrolysis [9].

This study aims to advance the field of bio-based materials by developing a PLA-based composite reinforced with CMC's citric acid-treated hemp. It provides a comparative analysis of cryo-milling and traditional methods, as well as CMC and $CaCO_3$ as fillers, emphasizing sustainable strategies for improving PLA's mechanical, thermal, and structural properties.

2. Materials and Methods

2.1. Materials

Degummed hemp fiber was acquired from Hemp Trader, Los Angeles, CA, USA (Product Code: F-DG1), Citric acid (Electrophoresis Grade, 99.5%) and Calcium carbonate (98%) were obtained from ThermoFisher (Waltham, MA, USA), and PLA (100 mesh) was obtained from Magerial Science.

2.2. Preparation of Cellulose Microcrystals (CMC)

To prepare cellulose microcrystals (CMC), five grams of oven-dried degummed hemp fibers, with diameters ranging from 5 to 80 microns, were cut into 0.5–1 cm length. These fibers were placed in three-necked, round-bottomed flasks containing 80% citric []]acid and distilled water under constant stirring. Hydrolysis was conducted at 100–110°C for two hours to ensure complete dissolution of the fibers. Once hydrolysis was complete, 400 mL of hot distilled water was added to terminate the reaction. The resulting suspension was filtered to remove excess acid and centrifuged three times using an Eppendorf Centrifuge 5810 R at 9289× g for 15 minutes per cycle. The suspension was dialyzed for 4–5 days to further eliminate residual acid, with the pH adjusted to 6–7, followed by a final centrifugation step. The resulting suspension was then dried to yield powdered cellulose microcrystals [9].

2.3. Size Reduction and Uniformity Enhancement of CMC Powder

CMC powder was cryo-milled (Retsch GmbH) individually to achieve a homogeneous fine particle size, reducing it from the microscale to the nanoscale. The powder was placed in the cryo-milling apparatus and processed for 5 minutes under cryogenic conditions using liquid nitrogen to maintain material brittleness and prevent agglomeration during milling.

2.4. Preparation of PLA-CNC Composites

PLA and CNC were combined in five different weight ratios (5%, 10%, 20%, 30%, and 40%). Two different processing methods were employed. In the cryo-milling method, PLA and CNC were cryo-milled together for 10 minutes under cryogenic conditions with liquid nitrogen to achieve

 doi:10.20944/preprints202504.1143.v1

uniform dispersion of CNC within the PLA matrix. In the physical mixing method, PLA and CNC powders were manually mixed as a control group.

2.5. Film Formation

Approximately 2 grams of each PLA-CNC composite was used to produce thin polymer films using a hot press. The press was set to a temperature of 175°C for 3 minutes, resulting in films with a 0.2–0.4 mm thickness. As you can see in Figure 1, the final films were uniform and suitable for further characterization.

2.6. Preparation and Film Formation of PLA-CaCO3 Composites

The same procedure described above for PLA-CNC composites was followed for PLA-$CaCO_3$ composites to maintain consistency across formulations. This approach allows for a direct comparison between CNC and $CaCO_3$ as reinforcement agents.

Figure 1. Film samples of 40% CNC/PLA composites with a millimeter scale (0–150 mm) for reference. The left film was produced through cryo-mixing, showing improved dispersion and uniformity, while the right film was prepared using physical mixing.

2.7. Characterization

2.7.1. Thermal Analysis

Thermal degradation of the films was evaluated using thermogravimetric analysis (TGA) with a TGA 550 instrument from TA Instruments (New Castle, DE, USA). Samples were heated to 600°C at a rate of 10°C/min under a nitrogen flow of 60 mL/min. The onset temperature of degradation (Td) was determined by ASTM E2550–11 standards. As shown in Figure 2, a representative TGA graph is provided as an example of a typical TGA run.

 doi:10.20944/preprints202504.1143.v1

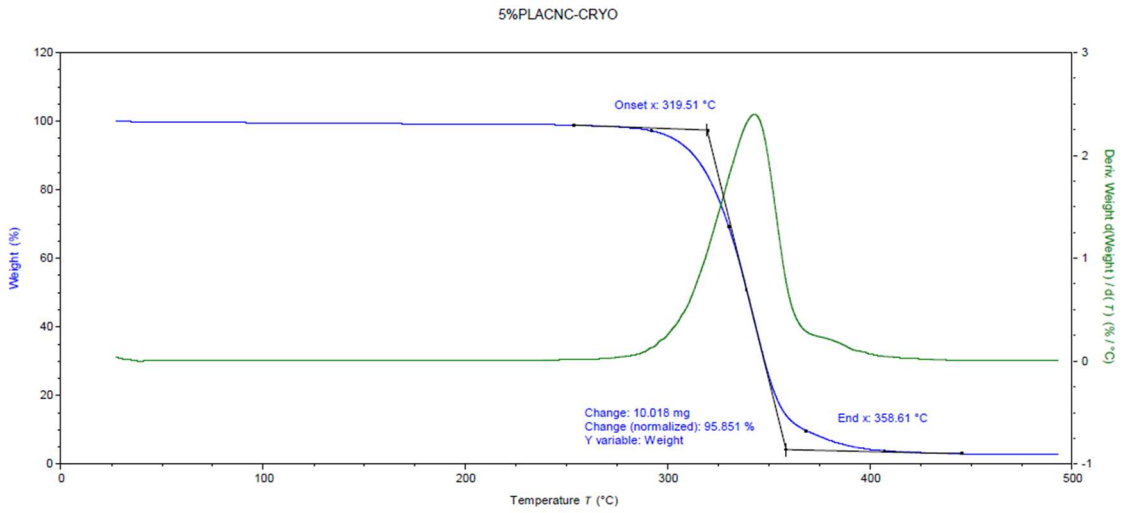

Figure 2. Thermogravimetric graph of 5% CNC/PLA film.

Differential scanning calorimetry (DSC) was conducted using a DSC 250 instrument (TA Instruments) to analyze the thermal properties of the films. The heat–cool–heat method was applied, cycling the temperature between 20°C and 200°C, remaining below the thermal degradation threshold of the samples. Heating and cooling rates were set at 10°C/min, with a 50 mL/min nitrogen flow rate maintained throughout the process. DSC analysis followed the ASTM D3418 standard for determining transition temperatures and enthalpies of fusion and crystallization of polymers, as indicated in Figure 3.

The degree of crystallinity was calculated as:

$$\mathbf{Xc} = \frac{\mathbf{\Delta Hm}}{\mathbf{w\Delta H0m}}$$

where ΔHm represents the enthalpy for the sample's melting point, ΔH0m is the enthalpy of melting for 100% crystalline PLA (93 J/g, as reported by Turner et al.[18]), and w signifies the weight fraction of PLA in the sample.

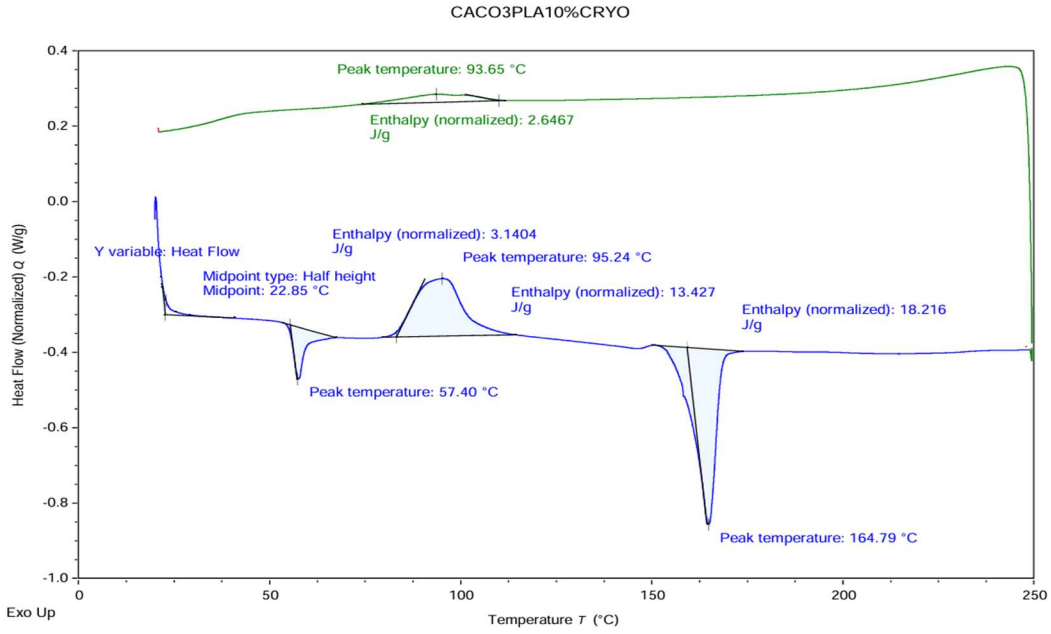

Figure 3. DSC graph of PLA film with 10% CaCo3.

 doi:10.20944/preprints202504.1143.v1

2.7.2. Mechanical Analysis

The mechanical properties of the films, including tensile strength, strain at maximum load, and Young's modulus, were assessed using a universal tensile testing machine (INSTRON 5543A, Norwood, MA, USA). The tests were conducted at a crosshead speed of 3.5 mm/min with a gauge length of 50 mm, following ASTM D882 standards. Six specimens (each 5 mm wide) were tested for each sample under controlled environmental conditions (20°C, 65% relative humidity). In total, 126 tests were performed across all samples. Figure 4 presents the graph obtained from the tensile strength test before converting the data from force to tensile stress for further analysis.

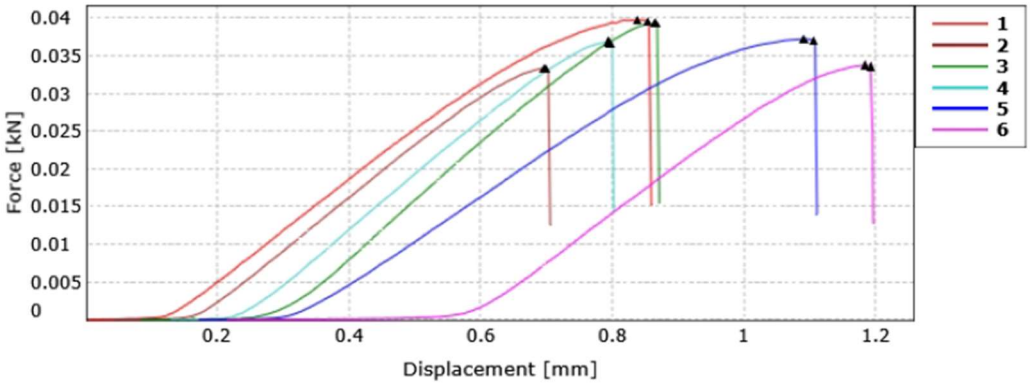

Figure 4. Tensile strength graph of PLA film with 5% CNC.

Sample names were abbreviated to indicate only the filler volume fraction and the mixing method for clarity and conciseness. The material type (PLA-CNC or PLA-$CaCO_3$) was omitted, as it is consistent across all samples. The sample naming convention follows this structure: [Filler Volume %]-[Mixing Method], where CRYO represents cryo-milled samples, and PHY represents physically mixed samples. For example, a 10% $CaCO_3$ sample prepared via cryo milling is denoted as 10%-CRYO, while a 20% CNC sample prepared by physical mixing is called 20%-PHY.

3. Results & Discussion

3.1. Thermal Characterization

3.1.1. TGA of CNC/PLA Film

Thermogravimetric analysis (TGA) was performed to evaluate the thermal stability of PLA and its biocomposite films, with results summarized in Table 1. The TGA curve, as shown in Figure 1, exhibits a single significant drop corresponding to the decomposition stage, primarily attributed to the thermal degradation of the polymer matrix, the evaporation of lightweight components, and the breakdown of polymer-filler interactions at elevated temperatures [21,22].

Table 1. Glass transition temperature (Tg), crystallization temperature (Tc), melting temperature (Tm), the heat of fusion (ΔHm), crystallinity degree (Xc), degradation temperature (Td), and Total Mass Change (TMC) of PLA and PLA/CNC Films.

Samples	Tg (°C)	Tc (°C)	Tm (°C)	ΔHm (J/g)	Xc (%)	Td (°C)	TMC (%)
PLA	57	94	167	37	40	311	66
5%-PHY	50	91	165	29	33	311	95
5%-CRYO	52	88	164	36	41	319	96

 doi:10.20944/preprints202504.1143.v1

10%-PHY	57	89	165	30	36	307	93
10%-CRYO	57	90	161	29	35	321	55
20%-PHY	56	89	162	26	35	311	93
20%-CRYO	61	92	166	29	39	311	72
30%-PHY	56	89	165	24	37	316	91
30%-CRYO	56	89	165	26	40	315	90
40%-PHY	60	92	164	22	39	316	65
40%-CRYO	58	92	167	32	57	316	91

According to the data presented in Table 1, no clear trend is observed in the decomposition temperature (Td). However, adding CNC to PLA generally stabilizes or slightly increases Td, except for the 10% physically blended sample, which exhibits a negligible decrease. The most significant increase in Td is observed in the 10% cryo-milled sample, reaching 321°C compared to 311°C for pure PLA, suggesting improved thermal stability. It has to be pointed out that the restricted movement of polymer chains caused by their attachment to nanocrystals may contribute to improved thermal stability, increasing chain rigidity and reducing susceptibility to oxidation and degradation reactions [23].

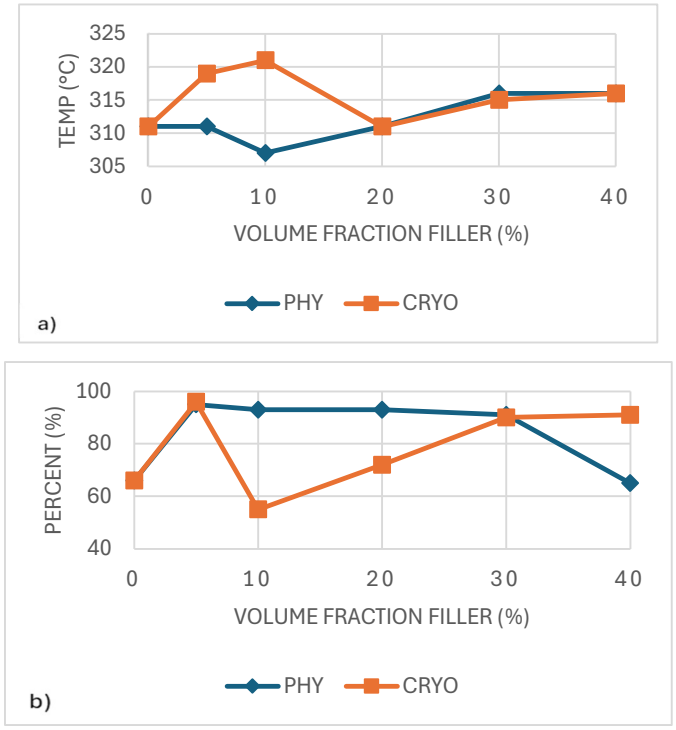

Figure 5. Degradation temperature (a), and total mass change (TMC) of CNC-PLA composites (b).

Similarly, as illustrated in Figure 5b, no distinct trend is observed for the total mass change. However, it is noteworthy that the 10% cryo-milled sample, which achieved the highest Td, also exhibits the lowest mass loss during decomposition. Cryo-milled samples generally demonstrate improved Td, indicating better thermal stability and reduced susceptibility to degradation than their physically mixed counterparts [24].

3.1.2. DSC of CNC/PLA Film

Differential scanning calorimetry (DSC) was used to determine the glass transition temperature (Tg), crystallization temperature (Tc), melting temperature (Tm), and crystallinity (Xc) of pure PLA and cellulose-reinforced biocomposite films, as shown in Table 1.

 doi:10.20944/preprints202504.1143.v1

As shown in Figure 6a, adding CNC generally lowered the glass transition temperature (Tg), especially at lower filler levels. This drop is attributed to increased chain mobility due to CNC interfering with how PLA chains are arranged, which allows the polymer chains to move more freely and transition at lower temperatures [25]. Cryo-milled samples consistently showed slightly higher Tg than physically mixed ones, likely due to better dispersion and tighter matrix interaction [26]. At 20% CRYO, Tg peaked, suggesting optimal filler-matrix interaction. Similar trends have been reported where dispersion and interfacial bonding influence thermal transitions [27].

Figure 6b shows that the amount of filler and the mixing method affected the PLA composites' crystallization temperature (Tc). Cryo-milled samples usually had higher Tc values than those made by physical mixing, likely because the CNCs were spread more evenly. This was most noticeable at 20% and 40% filler, where the Tc in the cryo-milled group went over 92°C. In comparison, the physically mixed samples had lower Tc values that did not change much, which means they did not help crystallization as much.

These findings suggest that better filler distribution increases the number of active nucleation sites, helping the material start crystallizing sooner as it cools. Similar findings have shown that nanocellulose can act as a crystallization promoter in PLA when well-integrated within the matrix [28–30].

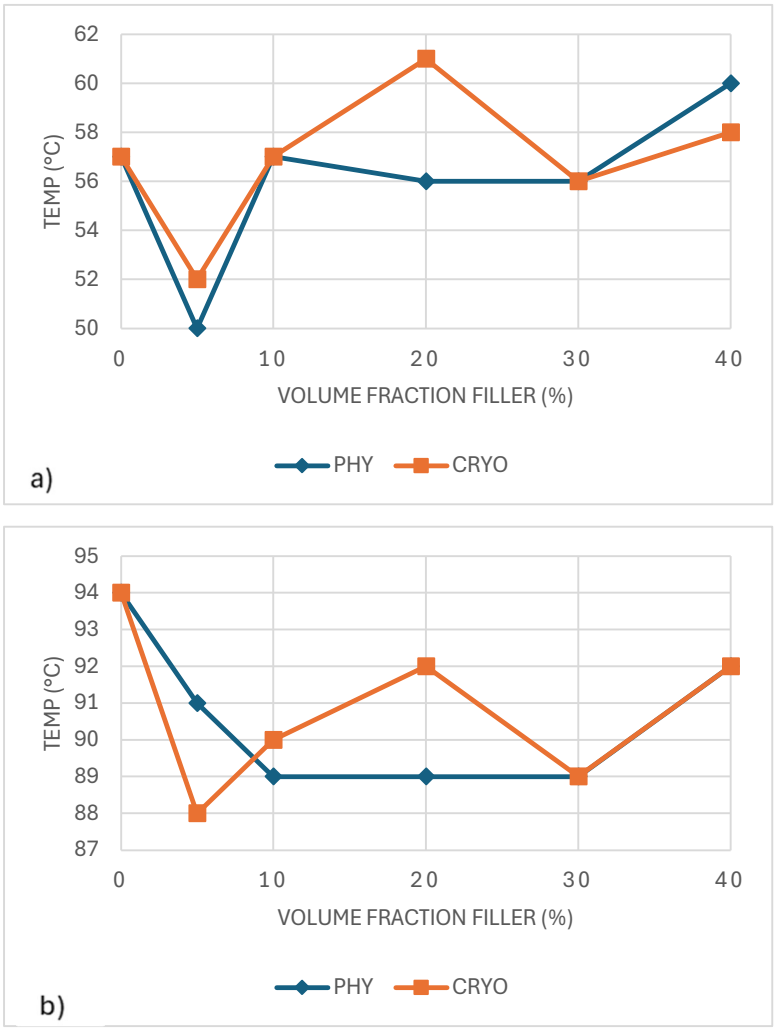

Figure 6. Glass transition temperature (a), and crystallization temperature (b) of CNC-PLA films.

As shown in Figure 7a, the PLA composites' melting temperature (Tm) stayed relatively steady across all filler contents, with values ranging from 161°C to 168°C. Small changes were seen in both processing methods, including a slight drop of around 10% filler, possibly due to less regular crystal

 doi:10.20944/preprints202504.1143.v1

formation at that level. Cryo-milled samples usually showed slightly higher Tm values than the physically mixed ones, likely because of better CNC distribution and more even crystal development. However, the differences were small. A similar pattern was reported by Lin et al. (2013), where CNCs had little effect on the melting point in PLA blends. This suggests that while CNCs may affect crystal structure, they do not significantly alter the thermal stability of the crystalline phase [29,31].

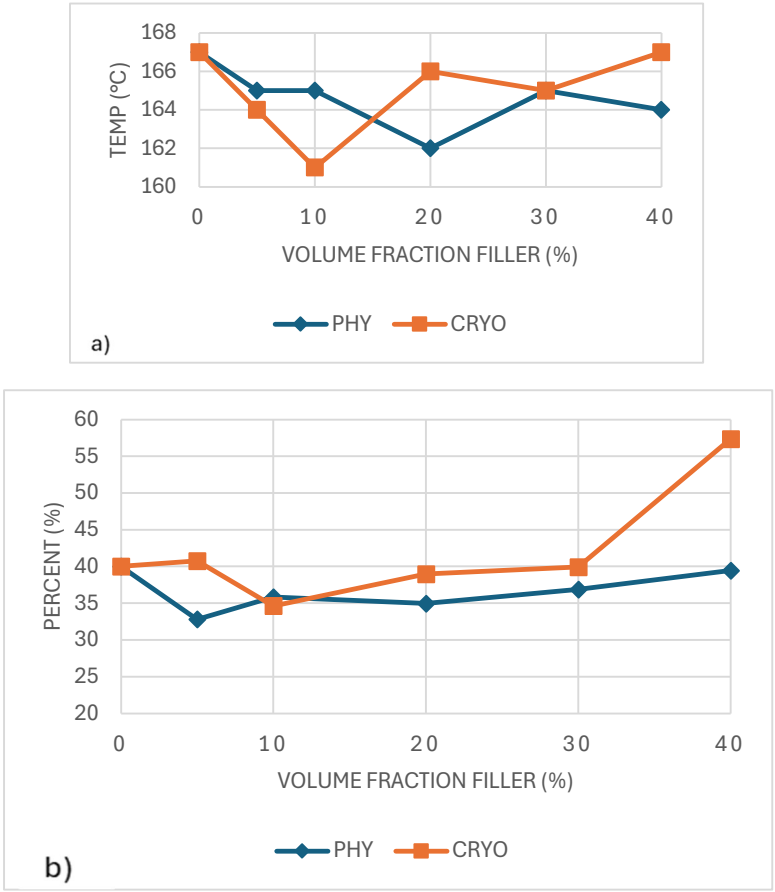

Figure 7. Melting temperature (a), and degree of crystallinity (b) of CNC-PLA films. .

As shown in Figure 7b, the degree of crystallinity (Xc) remained relatively consistent across all samples, with most values falling close to 40%, regardless of CNC content or mixing method. While a slight increase was observed in the 40%-CRYO sample, this variation is modest and could fall within the expected experimental error. These results suggest that although CNCs help initiate crystallization by providing nucleation sites, they do not significantly affect the total amount of crystalline structure that develops. In summary, CNCs appear to influence how quickly crystallization occurs rather than how much crystallinity is ultimately formed [32].

3.1.3. TGA of CaCO3/PLA Film

As shown in Table 2 and Figure 8a, the thermal degradation temperature (Td) decreases significantly with increasing $CaCO_3$ concentration. While pure PLA exhibits a Td of 311°C, the Td of 40%-CRYO drops drastically to 237°C. This decline suggests that $CaCO_3$ does not act as a thermal stabilizer but instead promotes degradation at higher loadings, aligning with literature findings [33]. Additionally, cryo-milled samples experience a more pronounced decline in Td than physically mixed samples, suggesting that improved dispersion leads to greater interfacial area, which may enhance susceptibility to thermal degradation at higher $CaCO_3$ loadings.

 doi:10.20944/preprints202504.1143.v1

Table 2. Glass transition temperature (Tg), crystallization temperature (Tc), melting temperature (Tm), the heat of fusion (ΔHm), crystallinity degree (Xc), degradation temperature (Td), and Total Mass Change (TMC) of PLA and PLA/CaCO3 Films.

Samples	Tg (°C)	Tc (°C)	Tm (°C)	ΔHm (J/g)	Xc (%)	Td (°C)	TMC (%)
PLA	57	94	167	37	40	311	66
5% -PHY	61	89	168	28	32	302	94
5% -CRYO	58	89	165	31	35	283	83
10% -PHY	60	92	165	28	33	275	86
10% -CRYO	57	95	165	18	22	264	80
20% -PHY	61	95	167	25	34	259	75
20% -CRYO	58	94	165	19	26	255	75
30% -PHY	61	95	166	20	31	266	67
30% -CRYO	59	98	165	17	26	246	68
40% -PHY	62	96	167	18	32	274	57
40% -CRYO	59	95	166	23	41	237	57

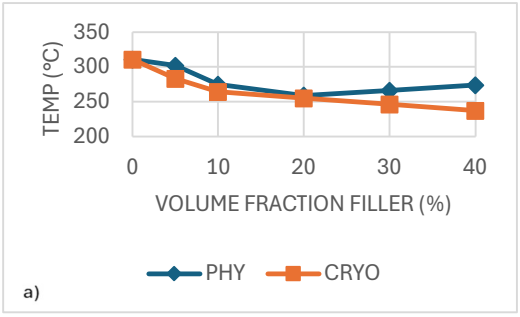

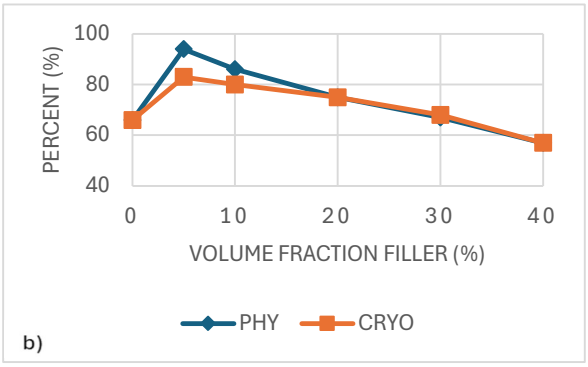

Figure 8. Degradation temperature (a), and total mass change (TMC) of CaCO3-PLA composites (b).

The total mass change (TMC) follows an inverse trend, with the mass loss being highest at lower $CaCO_3$ concentrations and gradually decreasing as filler content increases. The 5%-PHY sample undergoes the most significant mass loss (94%), while the 40%-CRYO sample retains more mass (57%). This suggests that higher $CaCO_3$ concentrations increase residual mass after decomposition, likely due to the formation of calcium-based thermal degradation byproducts. As shown in Figure 8, cryo-milled samples degrade at lower temperatures; they generally retain more mass at higher concentrations, as seen in the 40%-CRYO sample (57%) vs. the 5%-PHY sample (94%) [30].

 doi:10.20944/preprints202504.1143.v1

3.1.4. DSC of CaCO3/PLA Film

The glass transition temperature (Tg) of unreinforced PLA was about 57°C, as shown in Figure 9a and Table 2. In the physically mixed (PHY) samples, Tg shifted upward with the addition of $CaCO_3$, passing 60°C and continuing to rise slightly as more filler was added. This trend suggests that $CaCO_3$ particles make it harder for the PLA chains to move, which leads to a higher Tg. In contrast, the Tg of the cryo-milled (CRYO) samples stayed almost the same across all filler levels, remaining close to 57–59°C. This stability is likely due to the increased free volume introduced during cryo-milling, which improves chain mobility and offsets the stiffening effect of the filler. Similar behavior has been reported in PLA composites filled with inorganic particles, where shifts in Tg largely depend on the balance between particle dispersion and how well the filler bonds to the polymer matrix [34].

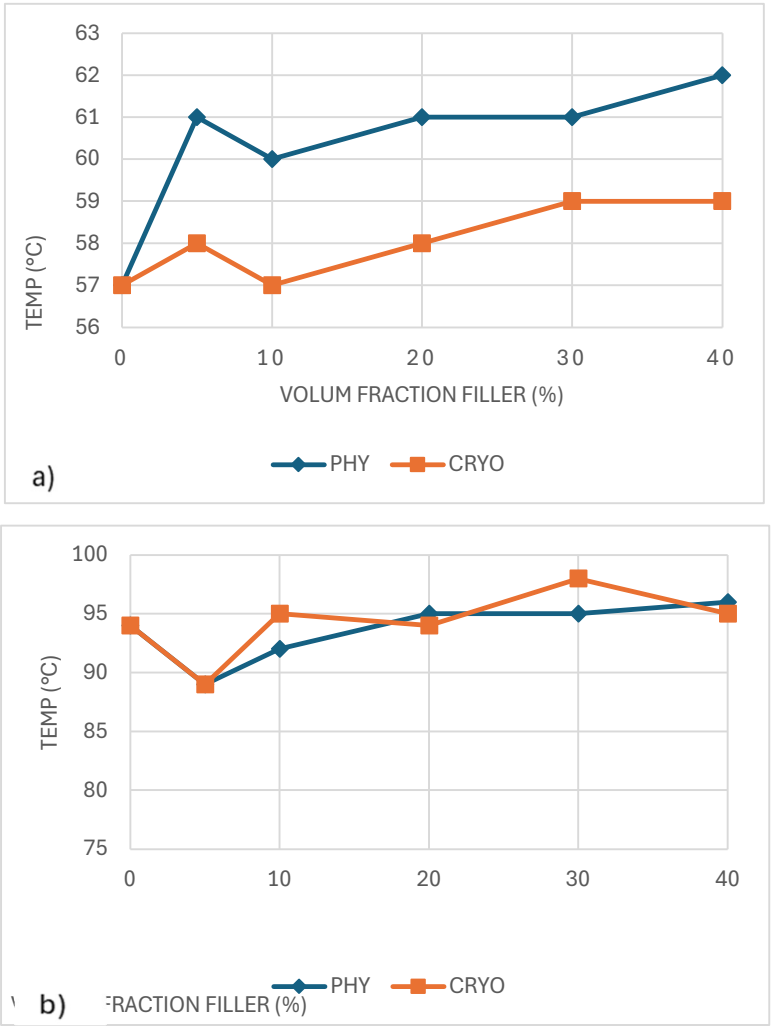

Figure 9. Glass transition temperature (a), and crystallization temperature (b) of CaCO3-PLA films.

Figure 9b shows how the crystallization temperature (Tc) changed with $CaCO_3$ addition. In the physically mixed (PHY) samples, Tc increased slightly as the filler content increased, suggesting that $CaCO_3$ acted as a as a modest nucleating agent. The cryo-milled (CRYO) samples showed a slightly more substantial effect, with Tc peaking around 98°C at 30% filler, likely due to better filler dispersion creating more places for crystals to start forming. Still, the overall changes were minor, meaning $CaCO_3$ helped crystallization happen faster but did not dramatically change the material's thermal behavior [35].

 doi:10.20944/preprints202504.1143.v1

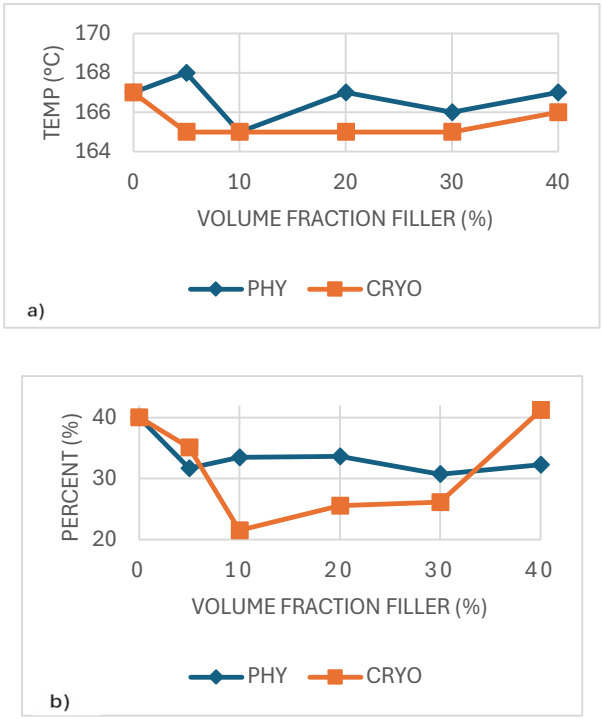

Figure 10. Melting temperature (a), and degree of crystallinity (b) of CaCO3-PLA films.

As shown in Figure 10a, the melting temperature (T_m) of PLA/$CaCO_3$/composites remains relatively stable across different filler concentrations, with only slight variations. The physically mixed (PHY) samples show a more noticeable fluctuation in T_m, and cryo-milled (CRYO) samples exhibit a more uniform trend, with T_m values consistently around 165–167°C, indicating that cryo-milling does not significantly alter the melting behavior of PLA. The overall stability of T_m across all samples suggests that $CaCO_3$ primarily affects crystallization behavior rather than significantly influencing the melting point of PLA [36].

The degree of crystallinity (Xc), as shown in Figure 10b, does not exhibit a consistent trend. In the physically mixed (PHY) samples, the crystallinity (Xc) degree remained constant, staying around 32–34% across all filler contents. In contrast, the cryo-milled (CRYO) samples showed a different behavior. Crystallinity dropped sharply to about 22% at 10% filler, then gradually increased with more filler. The most noticeable rise occurred at 40% filler, where Xc climbed to about 41%, slightly higher than that of unreinforced PLA. This pattern suggests that cryo-milling disrupted crystal formation at first but helped create more crystals when more $CaCO_3$ was added, probably by offering more places for the PLA chains to organize. Overall, $CaCO_3$ had a small but interesting effect on crystallinity, depending on both filler amount and how well it was dispersed [36,37].

The comparison of the thermal behavior between PLA/CMC and PLA/$CaCO_3$ is summarized in Table 3.

Table 3. Comparison between PLA/CMC and PLA/CaCO3 Thermal behavior.

Feature	CNC/PLA	$CaCO_3$/PLA	Observation
Tg	Slight decrease (more flexibility)	Slight increase (more rigidity)	CNC lowers Tg slightly by enhancing chain mobility, while $CaCO_3$ restricts chain motion, raising Tg.

 doi:10.20944/preprints202504.1143.v1

Tc	Noticeable increase (especially in CRYO samples)	Small to moderate increase (stronger in CRYO)	Both fillers promote nucleation; $CaCO_3$ shows a slightly stronger effect.
Xc	Relatively stable (~40%); slight increase at 40%-CRYO	Mostly stable (~32–34%); increases at 40%-CRYO	CNC better maintains or slightly improves crystallinity compared to $CaCO_3$, especially in CRYO samples.
Tm	Relatively unchanged (minor fluctuations)	Relatively unchanged (minor fluctuations)	Both fillers have minimal impact on melting temperature.
Td	Slight improvement with CNC addition	Slight decrease with $CaCO_3$ addition	CNC improves thermal degradation resistance; $CaCO_3$ tends to slightly lower it.
TMC	Lower mass loss (better thermal stability)	Higher mass loss	CNC helps retain more material mass at high temperatures compared to $CaCO_3$.

3.2. Mechanical Characterization

3.2.1. CNC/PLA Film

As shown in Figure 11a, the unfilled white bar represents unreinforced PLA, while the dark grey and light grey bars indicate physically mixed (PHY) and cryo-milled (CRYO) composites, respectively. The tensile strength of PLA significantly decreased with the addition of CNCs, regardless of the processing method. Unreinforced PLA exhibited the highest strength, around 40 MPa, while filled samples ranged between approximately 12 and 28 MPa. Physically mixed samples showed a sharper decrease across all filler levels, likely due to poor dispersion and weak bonding between PLA and CNC particles. Cryo-milled samples performed slightly better overall, suggesting that improved filler distribution helped reduce stress concentrations. Notably, the 40%-CRYO sample showed a clear boost in tensile strength compared to lower filler levels, reaching just under 30 MPa. This may be due to enhanced crystallinity and more effective load transfer at high filler content when dispersion is optimal. Similar reductions in tensile strength with CNCs have been reported and are often attributed to interfacial incompatibility and agglomeration in PLA matrices [28,38]. However, better dispersion techniques—such as cryo-milling or solvent exchange—can partially mitigate this effect.

As illustrated in Figure 11b, the colors are the same as previously described. The tensile strain of unreinforced PLA was the highest, around 3.4%, which shows that the material is more flexible. Once CNCs were added, strain values dropped across all samples, indicating a loss in flexibility. This drop is expected, as rigid fillers tend to **restrict** polymer chain mobility and introduce stress concentration points. However, cryo-milled samples consistently showed slightly higher strain values than their physically mixed counterparts at each filler level, suggesting that better dispersion helps maintain some ductility. Notably, the 40%-CRYO sample showed a modest recovery in strain,

 doi:10.20944/preprints202504.1143.v1

rising to over 2%, which may be attributed to improved particle distribution and reduced agglomeration at higher filler content. Previous studies have also shown that CNCs often reduce strain to failure in PLA, although proper dispersion can soften this effect by minimizing crack initiation zones [28,31].

Figure 11c follows the same color scheme used in the previous charts. The elastic modulus of unreinforced PLA was the lowest at around 1600 MPa. Once CNCs were added, the modulus increased in both physically mixed and cryo-milled samples, reaching values between 1900 and 2100 MPa. This overall increase is expected, as CNCs are rigid fillers that help reinforce the polymer matrix. Interestingly, the differences between PHY and CRYO samples were minimal across all filler levels. This might be because the modulus is mainly influenced by how much filler is added and how stiff the CNCs are rather than their bonding quality with the matrix. While changing the mixing method clearly improves CNC dispersion, it does not significantly enhance stiffness as long as the interface between filler and matrix remains weak. Similar observations have been made in other studies where PLA/CNC composites showed modest increases in modulus regardless of the dispersion method [39,40].

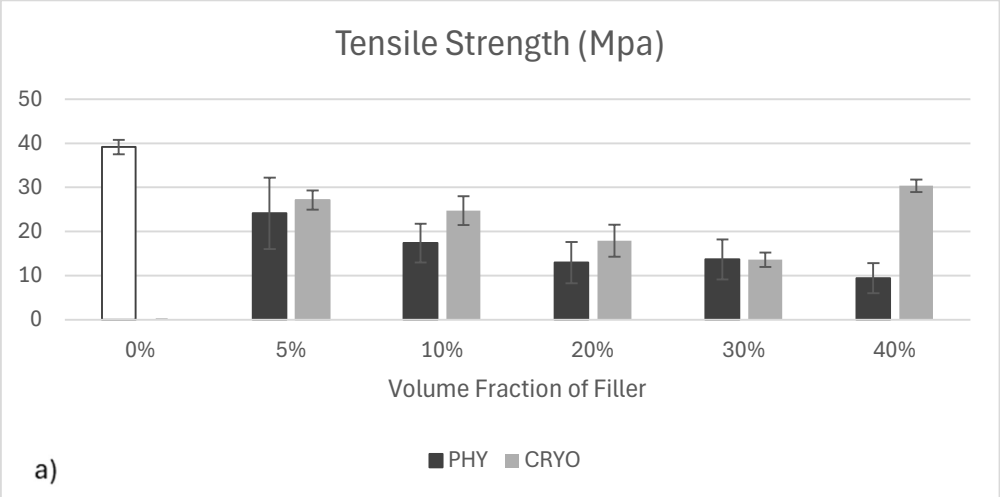

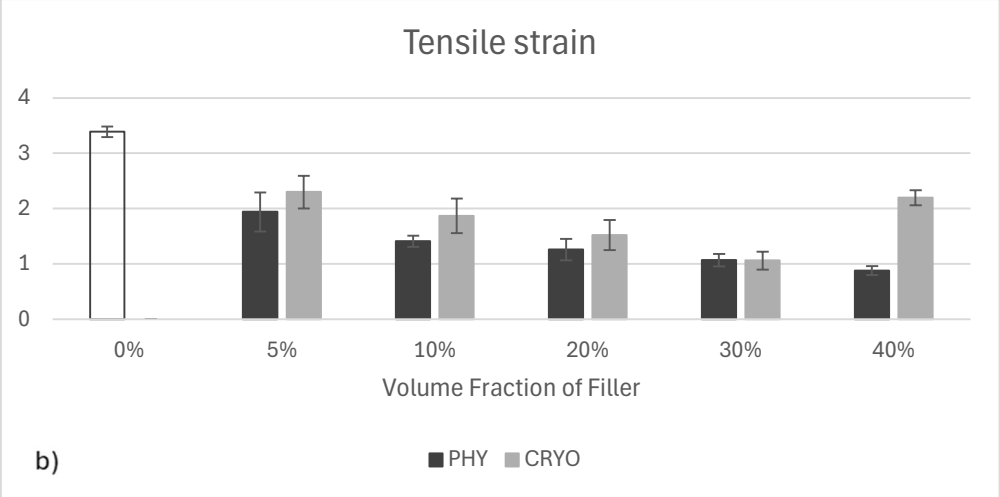

 doi:10.20944/preprints202504.1143.v1

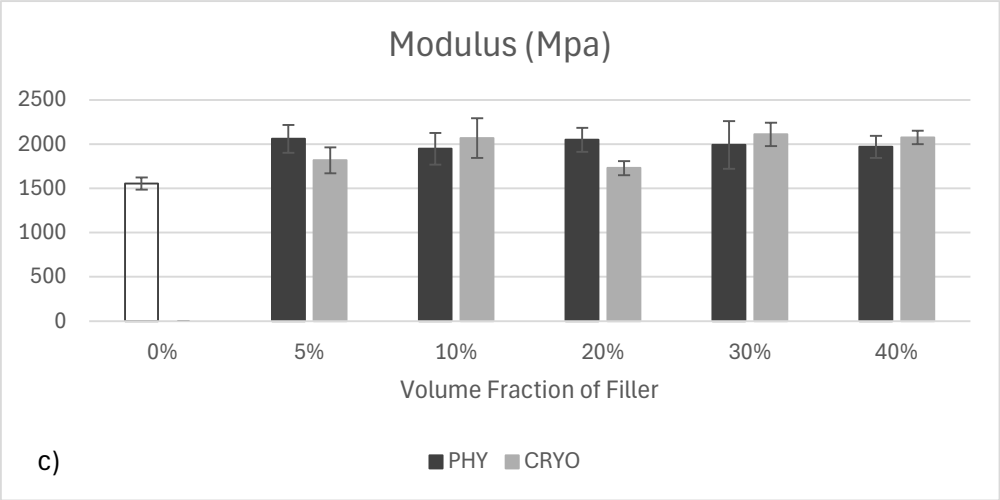

Figure 11. (a) Tensile strength, (b) tensile strain at maximum load, (c) Young's modulus of unreinforced PLA and CNC/PLA with physical and cryo-mill mixing. The error bars in the mechanical analysis graphs represent 95% confidence intervals (C.I.), indicating the variability and reliability of the measured data.

3.2.1. CaCO3/PLA Film

Figure 12a shows the effect of $CaCO_3$ addition on the tensile strength of PLA composites. The unfilled bar represents unreinforced PLA, while the dark grey and light grey bars correspond to physically mixed (PHY) and cryo-milled (CRYO) samples, respectively. Unreinforced PLA had the highest tensile strength, around 40 MPa. As $CaCO_3$ was added, tensile strength generally decreased across all filler contents. Physically mixed samples maintained slightly higher strength than cryo-milled ones, especially at lower filler levels. For example, at 5% and 10% filler, the physically mixed samples kept tensile strengths above 30 MPa, while the cryo-milled samples dropped more sharply. Both mixing methods showed a clear drop in strength at higher filler contents, especially at 30% and 40%, with values falling below 15 MPa. This suggests that although $CaCO_3$ can make the material stiffer, it also makes it weaker overall, likely because of poor bonding between the filler and the PLA and clumping of particles at higher loadings. Similar reductions in tensile strength with inorganic fillers have been observed in previous PLA composite studies [41,42].

Figure 12b shows how tensile strain changed with $CaCO_3$ addition. The colors are the same as previously described. Unreinforced PLA had the highest strain, around 3.5%, showing good flexibility. After adding $CaCO_3$, tensile strain dropped across all samples. Both PHY and CRYO samples showed a steady decrease as filler content increased, although physically mixed samples generally kept a slightly higher strain than the cryo-milled ones. The drop became more noticeable at 30% and 40% filler, where strain values fell below 1.5%. This behavior suggests that $CaCO_3$ makes the material more brittle by limiting the mobility of PLA chains and introducing stress points [43].

Figure 12c shows the changes in modulus with the addition of $CaCO_3$. The color scheme follows the same pattern described earlier. Unreinforced PLA had the lowest modulus, around 1500 MPa. After adding $CaCO_3$, modulus increased across all samples, especially for the physically mixed (PHY) composites [41,44,45]. PHY samples showed a steady rise in stiffness, reaching around 2800 MPa at 30% filler content. Cryo-milled (CRYO) samples also showed an improvement compared to unreinforced PLA, but their modulus was consistently lower than that of PHY samples at all filler levels. One possible reason for this difference is the particle size: $CaCO_3$ used in PHY samples was larger since it was not cryo-milled like the CRYO samples. Larger particles may have helped better reinforce the matrix, while the smaller cryo-milled $CaCO_3$ particles, combined with weaker interfacial bonding, made it harder to transfer stress effectively, leading to lower modulus. In short, when interfacial bonding is poor, using smaller particles can hurt stiffness rather than improve it [45].

 doi:10.20944/preprints202504.1143.v1

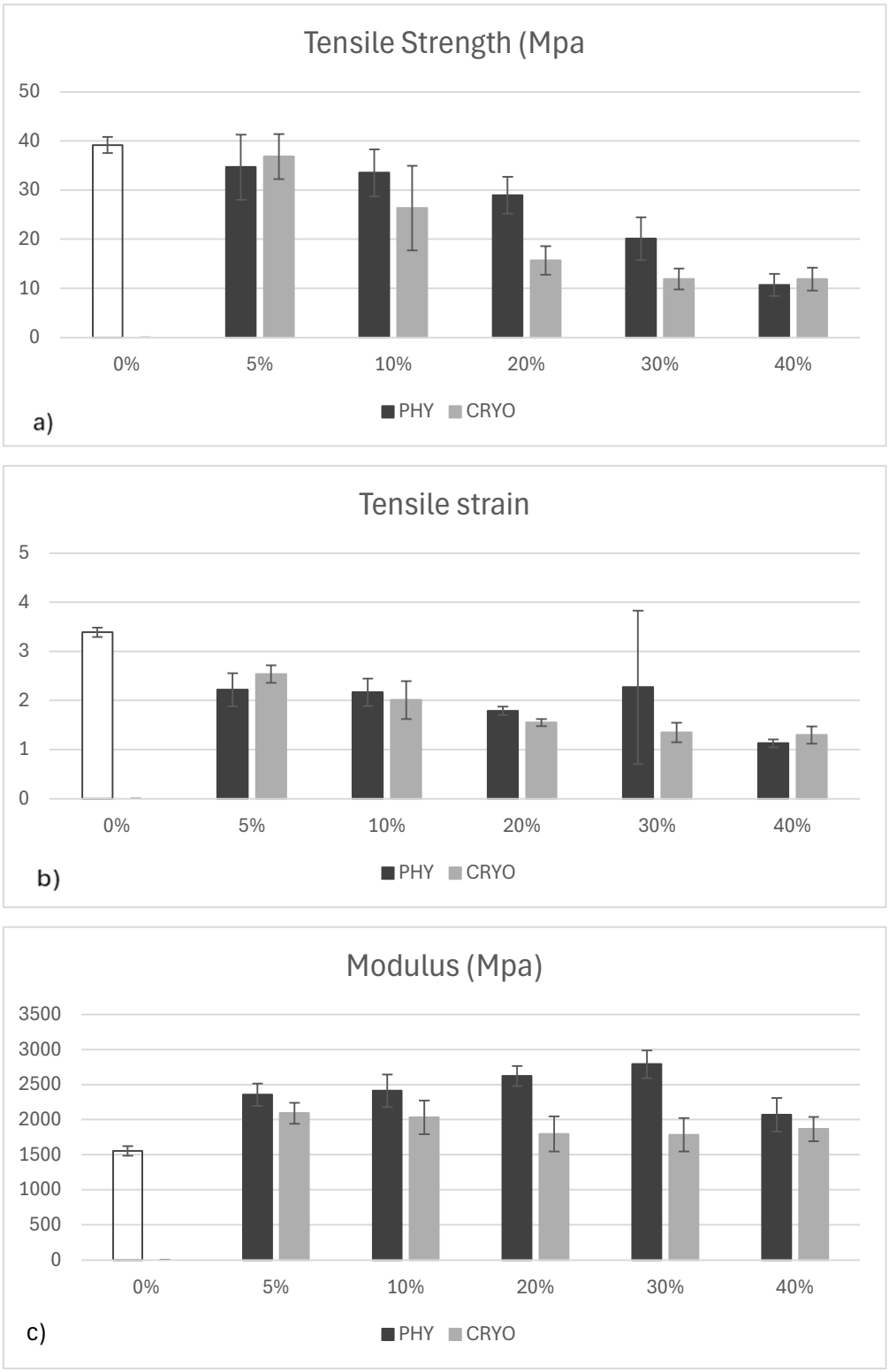

Figure 12. (a) Tensile strength, (b) tensile strain at maximum load, (c) Young's modulus of unreinforced PLA and CaCO3/PLA with physical and cryo-mill mixing. The error bars in the mechanical analysis graphs represent 95% confidence intervals (C.I.), indicating the variability and reliability of the measured data.

Table 4. Comparison between PLA/CMC and PLA/CaCO3 Composites Mechanical behavior.

Feature	CNC/PLA	$CaCO_3$/PLA	Observation

 doi:10.20944/preprints202504.1143.v1

Tensile Strength	Decreases with CNC addition; slight recovery at high filler (40%-CRYO)	Decreases steadily with $CaCO_3$ addition	CNC/PLA showed minor strength recovery at high loading (due to better dispersion), while $CaCO_3$/PLA continued weakening across all contents.
Tensile Strain	Drops significantly with CNC addition; better preserved in CRYO samples	Drops significantly with $CaCO_3$ addition; no major difference between PHY and CRYO	Both fillers reduce ductility, but CNC/PLA cryo-milling helps preserve strain slightly better than $CaCO_3$/PLA.
Modulus	Increases slightly with CNC addition; CRYO and PHY similar	Increases clearly with $CaCO_3$ addition; PHY samples show higher modulus than CRYO	$CaCO_3$ is more effective at boosting stiffness than CNC; particle size and interfacial bonding play important roles.

5. Conclusions

This study explored how adding cellulose nanocrystals (CNC) and calcium carbonate ($CaCO_3$) affects the properties of PLA composites, using both physical mixing and cryo-milling methods. The results showed that CNC and $CaCO_3$ influenced the composites differently in terms of thermal, mechanical, and structural behavior.

For thermal properties, CNC slightly lowered the glass transition temperature (Tg) by making the polymer chains more flexible, while $CaCO_3$ raised Tg, suggesting restricted chain movement. Both fillers helped speed up crystallization, as seen in the higher crystallization temperatures (Tc), with $CaCO_3$ having a slightly stronger effect. The degree of crystallinity (Xc) stayed stable for most samples, with small increases at higher filler contents. Neither filler had much effect on the melting temperature (Tm). Thermal degradation (Td) improved slightly with CNC but dropped a little with $CaCO_3$.

In terms of mechanical properties, both fillers reduced tensile strength and tensile strain, but CNC composites—especially those made with cryo-milling—retained more strength and ductility than $CaCO_3$ composites. On the other hand, modulus increased more with $CaCO_3$, especially in physically mixed samples. This difference seems to be linked to particle size and bonding: the larger $CaCO_3$ particles in physically mixed samples reinforced the matrix better, while the smaller cryo-milled particles, combined with weaker bonding, didn't boost stiffness as much. It's also important to mention that CNC powders had to be cryo-milled during lab preparation to create fine powders for processing. Meanwhile, $CaCO_3$ powders used for physical mixing were larger and not cryo-milled, which could partly explain why $CaCO_3$/PLA composites showed higher stiffness compared to CNC/PLA ones.

Overall, CNC was more effective at maintaining thermal stability and ductility, while $CaCO_3$ better-improved stiffness. Although cryo-milling helped improve filler dispersion in the PLA matrix, good dispersion alone wasn't enough to fully enhance mechanical performance. To improve load transfer and mechanical strength, surface modification of both CNC and $CaCO_3$ would be needed. These results highlight how important filler type, processing method, particle size, and filler–matrix interactions are when designing high-performance, sustainable PLA composites.

6. Future Work

Future studies should focus on improving the interfacial bonding between fillers and the PLA matrix through surface modification techniques. One promising approach is to modify the surface of CNC using polyethylene glycol (PEG), which could enhance compatibility with PLA and improve load transfer across the composite. Coating CNC with PEG may also help balance mechanical

 doi:10.20944/preprints202504.1143.v1

strength with flexibility, opening the door for developing more durable, bio-based composites. We are currently pursuing this direction by investigating PEG-modified CNC in PLA systems, and the results will be presented in a future publication.

Author Contributions: Conceptualization: F.M.B. and R.K.; writing—original draft preparation: F.M.B.; writing—review and editing: F.M.B., and R.K.; supervision: R.K.; funding acquisition: R.K. All authors have read and agreed to the published version of the manuscript.

Funding: This work was funded by Thomas Jefferson University through a foundation grant provided by the Lambert Innovation Fund.

Institutional Review Board Statement: Not applicable.

Informed Consent Statement: Not applicable.

Data Availability Statement: All data are presented in the manuscript.

Acknowledgments: The authors acknowledge…

Conflicts of Interest: The authors declare no conflicts of interest

References

1. S. Sinha Ray, '"Polylactide-Based Bionanocomposites: A Promising Class of Hybrid Materials," *Acc.Chem.Res.*, vol. 45, no. 10, pp. 1710–1720.
2. D. da Silva, M. Kaduri, M. Poley, O. Adir, N. Krinsky, J. Shainsky-Roitman and A. Schroeder, '"Biocompatibility, biodegradation and excretion of polylactic acid (PLA) in medical implants and theranostic systems," *Chemical engineering journal (Lausanne, Switzerland : 1996)*, vol. 340, pp. 9–14.
3. J. Lunt, '"Large-scale production, properties and commercial applications of polylactic acid polymers," *Polym.Degrad.Stab.*, vol. 59, no. 1, pp. 145–152.
4. R.E. Drumright, P.R. Gruber and D.E. Henton, '"Polylactic Acid Technology," *Advanced materials (Weinheim)*, vol. 12, no. 23, pp. 1841–1846.
5. K. Hamad, M. Kaseem, H.W. Yang, F. Deri and Y.G. Ko, '"Properties and medical applications of polylactic acid: A review," *Express polymer letters*, vol. 9, no. 5, pp. 435–455.
6. M. El Hajam, W. Sun, R. Hossain, I. Hafez, C. Howell and M. Tajvidi, '"Surfactant-assisted foam-forming of high performance ultra-low density structures made from lignocellulosic materials and cellulose nanofibrils (CNFs)," *Industrial crops and products*, vol. 221, pp. 119357.
7. Z. Wang, Z. Yao, J. Zhou, M. He, Q. Jiang, A. Li, S. Li, M. Liu, S. Luo and D. Zhang, '"Improvement of polylactic acid film properties through the addition of cellulose nanocrystals isolated from waste cotton cloth," *Int.J.Biol.Macromol.*, vol. 129, pp. 878–886.
8. J. Zhao, Y. Zhao, Z. Wang and Z. Peng, '"Effect of polymorphs of cellulose nanocrystal on the thermal properties of poly(lactic acid)/cellulose nanocrystal composites," *Eur.Phys.J.E*, vol. 39, no. 12, pp. 118–8.
9. F.M. Boroujeni, G. Fioravanti and R. Kander, '"Synthesis and Characterization of Cellulose Microfibril-Reinforced Polyvinyl Alcohol Biodegradable Composites," *Materials*, vol. 17, no. 2, pp. 526.
10. Y. Yin, J. Ma, X. Tian, X. Jiang, H. Wang and W. Gao, '"Cellulose nanocrystals functionalized with amino-silane and epoxy-poly(ethylene glycol) for reinforcement and flexibilization of poly(lactic acid): material preparation and compatibility mechanism," *Cellulose*, vol. 25, no. 11, pp. 6447–6463.

 doi:10.20944/preprints202504.1143.v1

11. M.J. Dunlop, R. Sabo, R. Bissessur and B. Acharya, "'Polylactic Acid Cellulose Nanocomposite Films Comprised of Wood and Tunicate CNCs Modified with Tannic Acid and Octadecylamine," *Polymers*, vol. 13, no. 21, pp. 3661.
12. Y. Zhang, C. Liu, M. Wu, Z. Li and B. Li, "'Impact of the Incorporation of Nano-Sized Cellulose Formate on the End Quality of Polylactic Acid Composite Film," *Nanomaterials (Basel, Switzerland)*, vol. 12, no. 1, pp. 1.
13. E.J. Lavernia, B.Q. Han and J.M. Schoenung, "'Cryomilled nanostructured materials: Processing and properties," *Materials science & engineering.A, Structural materials : properties, microstructure and processing*, vol. 493, no. 1, pp. 207–214.
14. A. Homavand, D.E. Cree and L.D. Wilson, "'Polylactic Acid Composites Reinforced with Eggshell/CaCO3 Filler Particles: A Review," *Waste*, vol. 2, no. 2, pp. 169–185.
15. K.P. Schlickmann, J.L.L. Howarth, D.A.K. Silva and A.P.T. Pezzin, "'Effect of The Incorporation of Micro and Nanoparticles of Calcium Carbonate in Poly (Vinyl Chloride) Matrix for Industrial Application," *Materials research (São Carlos, São Paulo, Brazil)*, vol. 22.
16. M. Rahmani, A. Adamian and Ahmad Hosseini-Sianaki, "'Effect of CaCO3 Nanoparticles on Vibrational Damping Behavior and Static Mechanical Properties of Polypropylene Composite Plates: An Experimental Investigation," *International journal of advanced design and manufacturing technology*, vol. 15, no. 1, pp. 85–94.
17. G. Kaur and R. Kander, "'System Dynamics for Manufacturing: Supply Chain Simulation of Hemp-Reinforced Polymer Composite Manufacturing for Sustainability," *Sustainability*, vol. 17, no. 2, pp. 765.
18. J.F. TURNER, A. RIGA, A. O'CONNOR, J. ZHANG and J. COLLIS, "'Characterization of drawn and undrawn poly-L-lactide films by differential scanning calorimetry," *Journal of thermal analysis and calorimetry*, vol. 75, no. 1, pp. 257–268.
19. E.M. Sullivan, R.J. Moon and K. Kalaitzidou, "'Processing and Characterization of Cellulose Nanocrystals/Polylactic Acid Nanocomposite Films," *Materials*, vol. 8, no. 12, pp. 8106–8116.
20. E. Lizundia, E. Fortunati, F. Dominici, J.L. Vilas, L.M. León, I. Armentano, L. Torre and J.M. Kenny, "'PLLA-grafted cellulose nanocrystals: Role of the CNC content and grafting on the PLA bionanocomposite film properties," *Carbohydr.Polym.*, vol. 142, pp. 105–113.
21. T.C. Mokhena, J.S. Sefadi, E.R. Sadiku, M.J. John, M.J. Mochane and A. Mtibe, "'Thermoplastic Processing of PLA/Cellulose Nanomaterials Composites," *Polymers*, vol. 10, no. 12, pp. 1363.
22. Monika, P. Dhar and V. Katiyar, "'Thermal degradation kinetics of polylactic acid/acid fabricated cellulose nanocrystal based bionanocomposites," *Int.J.Biol.Macromol.*, vol. 104, pp. 827–836.
23. S. Gazzotti, H. Farina, G. Lesma, R. Rampazzo, L. Piergiovanni, M.A. Ortenzi and A. Silvani, "'Polylactide/cellulose nanocrystals: The in situ polymerization approach to improved nanocomposites," *European polymer journal*, vol. 94, pp. 173–184.
24. S.S. Borkotoky, P. Dhar and V. Katiyar, "'Biodegradable poly (lactic acid)/Cellulose nanocrystals (CNCs) composite microcellular foam: Effect of nanofillers on foam cellular morphology, thermal and wettability behavior," *Int.J.Biol.Macromol.*, vol. 106, pp. 433–446.
25. M. Ruz-Cruz, P. Herrera-Franco, E. Flores-Johnson, M. Moreno-Chulim, L. Galera-Manzano and A. Valadez-González, "'Thermal and mechanical properties of PLA-based multiscale cellulosic biocomposites," *Journal of materials research and technology*, vol. 18, pp. 485–495.

 doi:10.20944/preprints202504.1143.v1

26. Y. Zhang, L. Cui, H. Xu, X. Feng, B. Wang, B. Pukánszky, Z. Mao and X. Sui, '"Poly(lactic acid)/cellulose nanocrystal composites via the Pickering emulsion approach: Rheological, thermal and mechanical properties," *Int.J.Biol.Macromol.*, vol. 137, pp. 197–204.
27. L. Szcześniak, A. Rachocki and J. Tritt-Goc, '"Glass transition temperature and thermal decomposition of cellulose powder," *Cellulose*, vol. 15, no. 3, pp. 445–451.
28. E. Fortunati, I. Armentano, Q. Zhou, A. Iannoni, E. Saino, L. Visai, L.A. Berglund and J.M. Kenny, '"Multifunctional bionanocomposite films of poly(lactic acid), cellulose nanocrystals and silver nanoparticles," *Carbohydr.Polym.*, vol. 87, no. 2, pp. 1596–1605.
29. M.P. Arrieta, E. Fortunati, F. Dominici, E. Rayón, J. López and J.M. Kenny, '"Multifunctional PLA–PHB/cellulose nanocrystal films: Processing, structural and thermal properties," *Carbohydr.Polym.*, vol. 107, pp. 16–24.
30. E. Lizundia, E. Fortunati, F. Dominici, J.L. Vilas, L.M. León, I. Armentano, L. Torre and J.M. Kenny, '"PLLA-grafted cellulose nanocrystals: Role of the CNC content and grafting on the PLA bionanocomposite film properties," *Carbohydr.Polym.*, vol. 142, pp. 105–113.
31. W.K. Ng, W.S. Chow and H. Ismail, '"Thermal properties enhancement of poly(lactic acid) by corn cob cellulose nanocrystals," *Polymers from renewable resources*, vol. 10, no. 4, pp. 63–76.
32. M.R. Kamal and V. Khoshkava, '"Effect of cellulose nanocrystals (CNC) on rheological and mechanical properties and crystallization behavior of PLA/CNC nanocomposites," *Carbohydr.Polym.*, vol. 123, pp. 105–114.
33. K. Piekarska, E. Piorkowska and J. Bojda, '"The influence of matrix crystallinity, filler grain size and modification on properties of PLA/calcium carbonate composites," *Polym.Test.*, vol. 62, pp. 203–209.
34. K. Piekarska, E. Piorkowska and J. Bojda, '"The influence of matrix crystallinity, filler grain size and modification on properties of PLA/calcium carbonate composites," *Polym.Test.*, vol. 62, pp. 203–209.
35. P. Srihanam, W. Thongsomboon and Y. Baimark, '"Phase Morphology, Mechanical, and Thermal Properties of Calcium Carbonate-Reinforced Poly(L-lactide)- b -poly(ethylene glycol)- b -poly(L-lactide) Bioplastics," *Polymers*, vol. 15, no. 2, pp. 301.
36. K. Piekarska, E. Piorkowska and J. Bojda, '"The influence of matrix crystallinity, filler grain size and modification on properties of PLA/calcium carbonate composites," *Polym.Test.*, vol. 62, pp. 203–209.
37. M. Sabzi, L. Jiang, M. Atai and I. Ghasemi, '"PLA/sepiolite and PLA/calcium carbonate nanocomposites: A comparison study," *J Appl Polym Sci*, vol. 129, no. 4, pp. 1734–1744.
38. J.L. Orellana, C.L. Kitchens, D. Wichhart and R. Nisticò, '"Mechanical and Optical Properties of Polylactic Acid Films Containing Surfactant-Modified Cellulose Nanocrystals," *Journal of nanomaterials*, vol. 2018, no. 2018, pp. 1–12.
39. E. Lizundia, E. Fortunati, F. Dominici, J.L. Vilas, L.M. León, I. Armentano, L. Torre and J.M. Kenny, '"PLLA-grafted cellulose nanocrystals: Role of the CNC content and grafting on the PLA bionanocomposite film properties," *Carbohydr.Polym.*, vol. 142, pp. 105–113.
40. Y. Zhang, L. Cui, H. Xu, X. Feng, B. Wang, B. Pukánszky, Z. Mao and X. Sui, '"Poly(lactic acid)/cellulose nanocrystal composites via the Pickering emulsion approach: Rheological, thermal and mechanical properties," *Int.J.Biol.Macromol.*, vol. 137, pp. 197–204.

 doi:10.20944/preprints202504.1143.v1

41. L. Aliotta, P. Cinelli, M.B. Coltelli and A. Lazzeri, "'Rigid filler toughening in PLA-Calcium Carbonate composites: Effect of particle surface treatment and matrix plasticization," *European polymer journal*, vol. 113, pp. 78–88.
42. J. Cisar, P. Drohsler, M. Pummerova, V. Sedlarik and D. Skoda, "'Composite based on PLA with improved shape stability under high-temperature conditions," *Polymer (Guilford)*, vol. 276, pp. 125943.
43. M. Bijarimi, S. Alya Azlan, M. Norazmi, E. Normaya and M.S.Z. Mat Desa, "'Sustainable green poly(lactic acid) (PLA)/eggshell powder (ESP) biocomposites," *Materials today : proceedings*, vol. 85, pp. 83–86.
44. V. Kumar, A. Dev and A.P. Gupta, "'Studies of poly(lactic acid) based calcium carbonate nanocomposites," *Composites.Part B, Engineering*, vol. 56, pp. 184–188.
45. D.K. Orisekeh, G. Corti and M.P. Jahan, "'Enhancing thermo-mechanical properties of additively manufactured PLA using eggshell microparticle fillers," *Journal of manufacturing processes*, vol. 133, pp. 782–797.